

Progression of Late-Onset Stargardt Disease

Stanley Lambertus,¹ Moritz Lindner,² Nathalie M. Bax,¹ Matthias M. Mauschwitz,² Jennifer Nadal,³ Matthias Schmid,³ Steffen Schmitz-Valckenberg,² Anneke I. den Hollander,^{1,4} Bernhard H. F. Weber,⁵ Frank G. Holz,² Gert Jan van der Wilt,⁶ Monika Fleckenstein,² and Carel B. Hoyng¹; for the Foveal sparing Atrophy Study Team (FAST)

¹Department of Ophthalmology, Donders Institute for Brain, Cognition and Behaviour, Radboud University Medical Center, Nijmegen, The Netherlands

²Department of Ophthalmology, University of Bonn, Bonn, Germany

³Institute for Medical Biometry, Informatics and Epidemiology, University of Bonn, Bonn, Germany

⁴Department of Human Genetics, Donders Institute for Brain, Cognition and Behaviour, Radboud University Medical Center, Nijmegen, The Netherlands

⁵Institute of Human Genetics, University of Regensburg, Regensburg, Germany

⁶Department for Health Evidence, Donders Institute for Brain, Cognition and Behaviour, Radboud University Medical Center, Nijmegen, The Netherlands

Correspondence: Carel B. Hoyng, Department of Ophthalmology, Radboud University Medical Center, P.O. Box 9101 (OHK400), 6500 HB Nijmegen, The Netherlands; carel.hoyng@radboudumc.nl

SL and ML are joint first authors.

MF and CBH contributed equally to the work presented here and should therefore be regarded as equivalent authors.

Submitted: April 28, 2016

Accepted: August 5, 2016

Citation: Lambertus S, Lindner M, Bax NM, et al.; for the Foveal sparing Atrophy Study Team (FAST). Progression of late-onset Stargardt disease. *Invest Ophthalmol Vis Sci.* 2016;57:5186–5191. DOI:10.1167/iovs.16-19833

PURPOSE. Identification of sensitive biomarkers is essential to determine potential effects of emerging therapeutic trials for Stargardt disease. This study aimed to describe the natural history of late-onset Stargardt, and demonstrates the accuracy of retinal pigment epithelium (RPE) atrophy progression as an outcome measure.

METHODS. We performed a retrospective cohort study collecting multicenter data from 47 patients (91 eyes) with late-onset Stargardt, defined by clinical phenotype, at least one *ABCA4* mutation, and age at disease onset ≥ 45 years. We analyzed RPE atrophy progression on fundus autofluorescence and near-infrared reflectance imaging using semiautomated software and a linear mixed model. We performed sample size calculations to assess the power in a simulated 2-year interventional study and assessed visual endpoints using time-to-event analysis.

RESULTS. Over time, progression of RPE atrophy was observed (mean: 0.22 mm/year, 95% confidence interval [CI]: 0.19–0.27). By including only patients with bilateral RPE atrophy in a future trial, 32 patients are needed to reach a power of 83.9% (95% CI: 83.1–84.6), assuming a fixed therapeutic effect size of 30%. We found a median interval between disease onset and visual acuity decline to 20/32, 20/80, and 20/200 of 2.74 (95% CI: 0.54–4.41), 10.15 (95% CI: 6.13–11.38), and 11.38 (95% CI: 6.13–13.34) years, respectively.

CONCLUSIONS. We show that RPE atrophy represents a robust biomarker to monitor disease progression in future therapeutic trials. In contrast, the variability in terms of the course of visual acuity was high.

Keywords: late-onset Stargardt, fundus autofluorescence, retinal pigment epithelium atrophy, biomarker, disease progression

Stargardt disease is an autosomal recessive retinal dystrophy caused by mutations in the *ABCA4* gene, and affects 1:8000 to 1:10,000 people worldwide.¹ Patients generally develop central loss of vision in childhood or early adulthood.^{2–4} However, late-onset Stargardt can be diagnosed at age ≥ 45 years, and has been associated with carrying one or two mutant *ABCA4* alleles.^{5,6} Patients with this late-onset variant may first present with metamorphopsia or oscillopsia without any decrease in visual acuity. Occasionally, these patients are asymptomatic and are incidentally diagnosed during screening tests for other retinal diseases, such as glaucoma, diabetes or thyroid disease.

The natural course of late-onset Stargardt includes a typical phenotype of yellow-white flecks and retinal pigment epithelium (RPE) atrophy. Patches of atrophy initially occur in the parafoveal retina and radially expand in size over time. New

atrophic areas can arise; multifocal atrophic areas coalesce. Atrophic areas can form a ring encircling the intact and still-functioning fovea. Then, it is only until late in the disease course that the fovea will be involved in the atrophic process.^{7–9} The patient's fixation point eventually shifts eccentrically, which leads to a substantial loss of visual acuity.¹⁰ However, central atrophy can also develop early in the disease course, and only minor disease progression has been described in other patients.⁵ Indeed, substantial variations in RPE atrophy progression have been reported before in small groups of typical Stargardt patients.¹¹ Yet analyses of the natural course of large late-onset Stargardt cohorts are missing.

In light of recently upcoming therapeutic options for Stargardt disease,^{12–14} accurate biomarkers to determine their potential effects are crucial. The well-defined area of RPE atrophy is a frequent feature of late-onset Stargardt, showing



similarities to geographic atrophy in age-related macular degeneration (AMD). Fundus autofluorescence (FAF) imaging can clearly visualize such areas of RPE atrophy,^{15,16} and change in RPE atrophy over time by FAF has already been accepted as a clinical endpoint by the U.S. Food and Drug Administration in AMD.¹⁷ We hypothesize that areas of RPE atrophy could also serve to sensitively monitor the effect of a drug trial in late-onset Stargardt. This would make patients with late-onset Stargardt appropriate candidates for upcoming therapeutic trials. In this study, we describe the natural history in late-onset Stargardt patients, and identify cohorts based on imaging parameters that determine the visual course in these patients. We quantify atrophy progression with semiautomated software, previously validated for AMD,¹⁸ showing the accuracy of this outcome measure, and include sample size calculations that are valuable for the design of upcoming therapeutic trials.

METHODS

Patient Selection

We identified patients from the Stargardt database of the Department of Ophthalmology at Radboud University Medical Center (Nijmegen, The Netherlands) and from the participants in the prospective natural history study Fundus Autofluorescence in Age-related Macular Degeneration (FAM; NCT00393692).

We included 47 patients with a late disease onset, defined by an age ≥ 45 years at which symptoms were first noticed.⁵ If the patient did not report any symptoms, we used the age at which the patient was diagnosed by an ophthalmologist. We clinically considered patients to have late-onset Stargardt when typical yellow-white flecks or dots were seen that correlated with hyperautofluorescent flecks on 488-nm FAF imaging.

Patients were analyzed for the presence of mutations in the ATP-binding cassette, subfamily A, member 4 (*ABCA4*, NM_000350.2) gene. Clinical diagnosis was confirmed by genetic testing if at least one *ABCA4* mutation was found. We excluded patients without evidence of *ABCA4* mutations. In patients carrying only one *ABCA4* mutation, we performed additional sequencing of the peripherin-2 gene (*PRPH2*, NM_000322.4) to exclude pseudo-Stargardt pattern dystrophy and central areolar choroidal dystrophy.^{19,20}

This cohort study was carried out with approval from the Institutional Ethics Committee at Radboud University Medical Center (Nijmegen, The Netherlands) and the University Hospital of Bonn (Bonn, Germany), and adhered to the tenets of the Declaration of Helsinki. All patients provided informed consent before giving a blood sample and receiving additional ophthalmologic examinations to complete the clinical assessment.

Clinical Assessment

We reviewed the patients' records for ophthalmologic history and available technical examinations, including sex, age at disease onset, and age at baseline. Best-corrected visual acuity (BCVA) was measured using a Snellen or Early Treatment Diabetic Retinopathy Study (ETDRS) chart, then transformed into the logarithm of the minimum angle of resolution (logMAR) for subsequent analysis. Fundus characteristics were documented using fundus photography (Topcon TRC-50IX; Topcon Corporation, Tokyo, Japan; or Visucam 500; Carl Zeiss Meditec, Jena, Germany). Fundus autofluorescence ($\lambda = 488$ nm; emission 500–700 nm) and near-infrared reflectance (NIR; $\lambda = 820$ nm) imaging were performed using a confocal scanning laser ophthalmoscope (Spectralis HRA+OCT or

HRA2; Heidelberg Engineering, Heidelberg, Germany) in a subset of visits. The field of view was set at $30^\circ \times 30^\circ$ or $55^\circ \times 55^\circ$ and was centered on the macula. Eyes with signs of choroidal neovascularization were excluded from further analysis.

Image Grading and Cohorts

For each visit, two independent graders (MF and ML), blinded to each other's results, evaluated the status of the fovea and the presence of clearly demarcated RPE atrophy (analogous to "definitely decreased autofluorescence," the term recently used by Kuehlewein et al.²¹) on all available imaging modalities. Atrophy was graded as follows: (1) no RPE atrophy with an intact fovea, (2) extrafoveal (but not fovea encircling) RPE atrophy, (3) a typical "foveal sparing" phenotype in which RPE atrophy encircled the fovea by $\geq 180^\circ$,¹⁰ or (4) foveal involvement. Foveal involvement was indicated by a mottled or absent autofluorescent signal (equaling what was ultimately termed "well/poorly demarcated questionably decreased autofluorescence"²¹). In cases of discrepancy, a third grader (SL) evaluated the images. His agreement with one of the independent graders was finally used. Based on this grading, eyes were exploratively analyzed in order to form cohorts that might be predictive for visual acuity loss.

Quantitative Measurements of Retinal Pigment Epithelium Atrophy

Two independent graders (MF and ML), blinded to each other's results, performed measurements of the area of RPE atrophy using the RegionFinder software (version 2.5.5.0, Heidelberg Engineering) on FAF images, as previously established for AMD.¹⁸ In cases in which the foveal borders of the atrophy could not be well determined in FAF images, NIR images were included in the analysis wherever available.²² The final value was defined as the average of the two measurements between the readers, provided that the two measurements did not differ by >0.15 mm². If the difference exceeded 0.15 mm², a senior reader (MMM) additionally performed the measurement.¹⁸ We calculated the final value by averaging the senior reader measurement along with the closer of the two other reader measurements.

Statistical Analysis

We analyzed data using SAS Statistical Analysis Software Version 9.2 (SAS Institute, Cary, NC, USA) and R Version 3.1.2.²³ Supplementary Figure S1 gives an overview of the analytical process applied in this work. Changes in visual acuity over time were assessed by time-to-event curves (cumulative distribution functions), and atrophy progression was analyzed using linear mixed-effects models. We performed a simulation study for power calculation for possible future interventional trials. Unless otherwise stated, all values given in the text represent median, minimum, and maximum values. Groups were compared by Mann-Whitney *U* tests. Details on the statistical procedures can be found in Supplementary Text S1.

RESULTS

Patient Features and Initial Symptoms

A total of 91 eyes of 47 patients (19 men, 28 women) were included in this study. Two mutations in the *ABCA4* gene were found in 20 patients (42.6%) and one mutation in 27 (57.4%; Supplementary Table S1). The median age at disease onset was

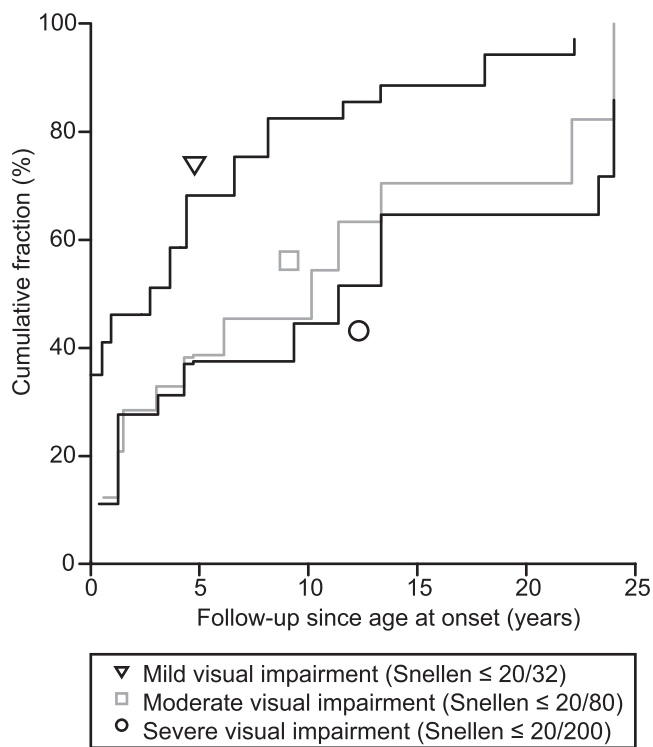


FIGURE 1. Time-to-event curve (computed as 1 minus the Turnbull estimates) showing the cumulative fraction of eyes in late-onset Stargardt patients reaching the following clinical endpoints: mild visual impairment (≥ 0.2 logMAR, Snellen \leq 20/32; *triangle*), moderate visual impairment (≥ 0.6 logMAR, Snellen \leq 20/80; *square*), and severe visual impairment (≥ 1.0 logMAR, Snellen \leq 20/200; *circle*). logMAR, logarithm of the minimum angle of resolution.

54 years (range, 45–84). Self-reported initial symptoms were obtained for 42 patients and included a decrease in visual acuity ($n = 24$; 50%), metamorphopsia ($n = 12$; 29%), nyctalopia ($n = 5$; 12%), paracentral scotomas ($n = 4$; 10%), or oscillopsia ($n = 1$; 2%). Twelve patients (29%) did not report any visual complaints. In five patients, initial symptoms were not unequivocally denoted in the patient’s file.

Course of Visual Acuity

Overall, visual acuity data were available from 632 eye visits. At the first presentation after disease onset, the median disease duration was 0.9 years (range, 0–25.6) with a median BCVA of 0.10 logMAR (range, -0.14 to 1.70; Snellen 20/25). The median follow-up time of the patients with more than a single visit (45 out of 47 patients) was 4.8 years (range, 0.04–25.0). Time-to-event analysis yielded a median and 95% confidence interval (CI) between the age at onset and a decline in BCVA to mild visual impairment ($n = 62$), moderate visual impairment ($n = 39$), and severe visual impairment ($n = 35$) of 2.74 (0.54–4.41), 10.15 (6.13–11.38), and 11.38 (9.34–13.34) years, respectively (Fig. 1). The median disease duration at the final visit was 6.8 years (range, 0–30.9). The median BCVA at the final visit was 0.37 logMAR (range, -0.10 to 1.80; Snellen 20/47).

Assessment of Retinal Features

For each patient, clinical imaging data were available for a subset of visits (241 eye visits of 91 eyes). At baseline (first visit with imaging data available), yellow-white flecks were observed in all but one patient, in whom small yellowish spots were noted. An apparently intact fovea (Fig. 2A) without mottled or sharply decreased autofluorescence indicating RPE atrophy was present in 58 eyes. Out of these 58 eyes without foveal involvement, 22 had no RPE atrophy (Fig. 2B), 16 had extrafoveal (but not fovea encircling) atrophy (Fig. 2C), and 20

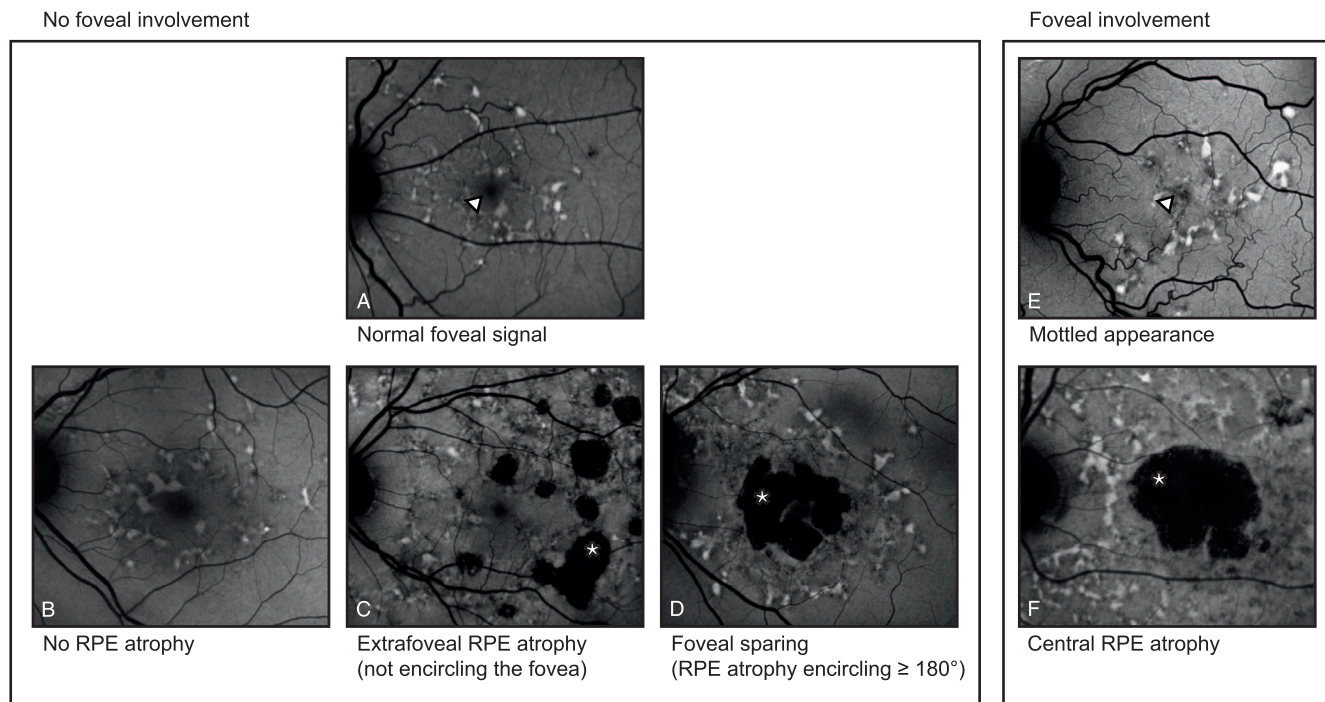


FIGURE 2. The assessment of retinal features in late-onset Stargardt patients was done by grading foveal involvement and RPE atrophy. The foveal signal (*triangles*) was graded as either (A) “uninvolved/normal” or (E) “involved” (mottled or absent). RPE atrophy (*asterisks*) was graded as (B) none, (C) extrafoveal (but not fovea encircling), (D) foveal sparing ($\geq 180^\circ$ encircling the fovea), or (F) central RPE atrophy. RPE, retinal pigment epithelium.

TABLE 1. Retinal Features in Late-Onset Stargardt Over the Entire Observational Interval

At Baseline			Clinical Course		
Initial Features	Eyes	Median Visual Acuity, logMAR (Range)	Change in Features	Median Visual Acuity, Final Visit, logMAR (Range)	Resulting Cohort
No foveal involvement					
No RPE atrophy	22	0.10 (−0.20 to 0.64)	20 unchanged	0.06 (−0.06 to 0.58)	I
			2 eyes developed extrafoveal atrophy	−0.02 (−0.06 to 0.02)	II
Extrafoveal but not fovea encircling	16	0.05 (−0.10 to 0.72)	9 unchanged	0.12 (0 to 1.54)	II
			6 progressed to foveal sparing	0.44 (−0.06 to 0.74)	III
			1 developed foveal involvement	0.36	IV
Foveal sparing encircling ≥ 180°	20	0.12 (0 to 0.52)	16 unchanged	0.22 (−0.04 to 1.80)	III
			4 eyes loss of foveal sparing	1.25 (0.94 to 1.50)	III
Foveal involvement					
Central RPE atrophy	9	0.98 (0.30 to 1.50)		1.10 (0.80 to 1.50)	IV
Mottled	23	0.30 (−0.08 to 1.80)	20 eyes unchanged	0.69 (−0.10 to 1.72)	IV
			3 eyes changed to central RPE atrophy	1.30 (1.10 to 1.80)	IV

Cohort I had only flecks without any mottled foveal alterations or RPE atrophy; cohort II had extrafoveal (but not fovea encircling) RPE atrophy until the last visit; cohort III developed foveal sparing (RPE atrophy encircling the fovea ≥ 180°); and cohort IV had foveal involvement by either a mottled fovea or central RPE atrophy without passing through a foveal sparing phenotype during the observational interval.

had a foveal sparing pattern of RPE atrophy encircling the fovea ≥ 180° (Fig. 2D). The other 32 eyes had an involved fovea by either a mottled appearance (23 eyes; Fig. 2E) or central RPE atrophy (9 eyes; Fig. 2F). One eye was excluded because it was inconclusive if the fovea appeared mottled. There was no significant difference in patient’s age between eyes that initially had foveal involvement and those that did not (median: 60.4 [n = 32] and 61.0 years [n = 58], respectively; P = 0.421).

Cohorts

Assessment of retinal features over the entire imaging interval (Table 1) enabled us to categorize the eyes into four clearly distinctive cohorts. During the entire follow-up period, 20 eyes (22.2%) showed only flecks without any mottled foveal alterations or RPE atrophy (cohort I). Eleven eyes (12.2%) showed extrafoveal (but not fovea encircling) RPE atrophy (cohort II). Twenty-six eyes (28.9%) developed foveal sparing (RPE atrophy encircling the fovea ≥ 180°; Cohort III). In four of these 26 eyes, the fovea eventually involved in the atrophic process at the last visit. Thirty-three eyes (36.7%) had eventual foveal involvement without passing through a foveal sparing phenotype during the observational interval (cohort IV).

The median follow-up periods of the entire imaging interval of cohorts I, II, III, and IV were 3.4 (range, 0–10.4), 3.3 (range, 0.1–11.7), 8.7 (range, 2.1–30.9), and 11.4 (range, 0.3–30.9) years, respectively. Eyes in cohorts I and II had a median disease duration of 3.4 years (range, 0–11.7), which was shorter (P = 1.0 × 10^{−6}) than in cohort III and IV (median: 11.0 years; range, 0.3–30.9).

Based on the morphologic observation of distinct cohorts among collective late-onset Stargardt patients, we further analyzed eyes with long follow-up grouped into the “foveal sparing” (cohort III) and “foveal involvement” (cohort IV) cohorts for possible distinctive long-term visual courses among these cohorts. Eyes that formed foveal sparing cohort III took an overall favorable visual course when compared to eyes from foveal involvement cohort IV. Survival analysis for the endpoints ≥ 0.2 logMAR, ≥ 0.6 logMAR, and ≥ 1.0 logMAR showed a notably later, though not significant, occurrence of each of these events in eyes from foveal sparing cohort III (Table 2).

Modeling of Retinal Pigment Epithelium Atrophy

We assessed changes in RPE atrophy area over time in a subset of visits from 66 eyes (from 21 female and 17 male patients). The median follow-up time with FAF imaging was 2.3 years (range, 0.07–7.7). Measurement of RPE atrophy size was possible with high agreement between two independent readers (Supplementary Fig. S2). At the first visit, the mean RPE atrophy size was 6.26 mm² (± standard deviation: 7.3). Square root transformed data were used for all further analysis. Modeling RPE atrophy over time revealed an annual atrophy progression rate (slope) of 0.22 mm²/year (95% CI: 0.19–0.27).

For 28 patients, data on RPE atrophy progression were available from both eyes for the same observational interval, and revealed that atrophy progression rates moderately correlated between the two eyes of a single patient (Pearson’s r = 0.52; Supplementary Fig. S3).

TABLE 2. Median Times (Years; 95% Confidence Interval) of Best-Corrected Visual Acuity Decline Since the Age at Onset Compared Between Eyes of Late-Onset Stargardt Patients Who Developed Foveal Sparing and Those Who Had Early Foveal Involvement

Cohort	Mild Impairment ≤ 20/32, ≥ 0.2 logMAR	Moderate Impairment ≤ 20/80, ≥ 0.6 logMAR	Severe Impairment ≤ 20/200, ≥ 1.0 logMAR
Foveal sparing, cohort III	0.95 (NA*–6.61) years	10.15 (3.09–13.34) years	23.3 (13.6–NA*)
Foveal involvement, cohort IV	0.51 (NA*–4.41) years	7.73 (4.30–22.89) years	NA* (24.0–N/A*)
Log-rank test	0.57	0.07	0.06

NA, not available.

* Values could not be calculated, as too many events occurred outside the observational interval.

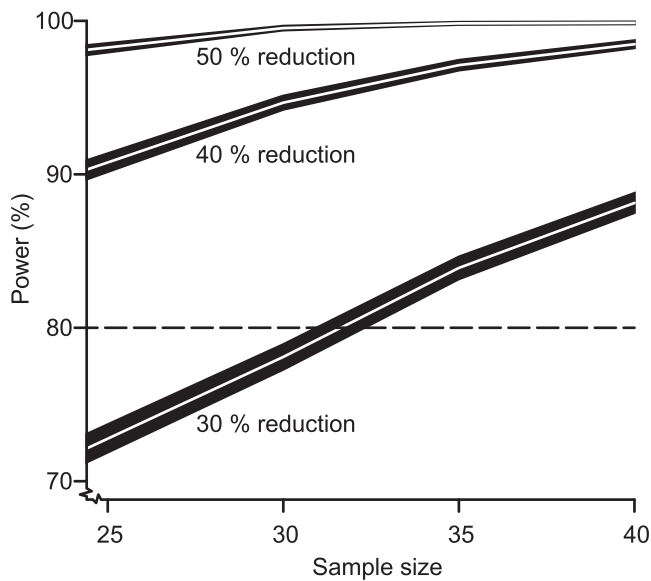


FIGURE 3. Statistical power as a function of sample size. Calculations were performed for expected effect sizes of 50%, 40%, and 30% reduction of atrophy progression. The figure shows the power values \pm 95% confidence intervals for each value of the effect size, as estimated from a simulation study with 10,000 runs. The significance level was set to 0.05. A trial duration of 2 years was assumed.

Sample Size Calculations

Based on the observed progression kinetics and the agreement between two eyes of a single individual, we were able to perform sample size calculations for possible future therapeutic trials. The assumption of a trial duration of 2 years and inclusion of only patients with bilateral RPE atrophy resulted in the sample size–power relationship depicted in Figure 3, with expected effect sizes of 50%, 40%, and 30% reduction in RPE atrophy progression. For effect sizes of 50% and 40%, fewer than 25 patients would be needed to obtain a statistical power of 0.9 at the 5% significance level, while for an effect size of 30%, a power of 0.8 would be reached if at least 32 patients were included.

DISCUSSION

The natural history of late-onset Stargardt features expanding, well-demarcated areas of RPE atrophy, which can be a promising clinical biomarker to monitor disease progression. Although clinical features have been previously described,⁵ we comprehensively report on visual course and specific RPE atrophy progression rates in a large multicenter cohort that was well defined by clinical, genetic, and validated imaging parameters. In addition, we used advanced statistical methods to deliver robust results,^{24,25} as these are required for planning and conducting clinical trials. These measures ensured the highest levels of data integrity. As a result, this work showed that a future therapeutic trial can be realized with sufficient statistical power with a cohort of as few as 35 patients (Fig. 3).

In contrast, visual acuity loss may not be a useful outcome measure in clinical trials due to its high interindividual variance² and overall slow decline; this would result in unrealistic large cohorts and long follow-up. Surrogate biomarkers may be more convenient, ideally predicting long-term changes in functional disease progression by detecting small short-term changes.²³ Indeed, both visual acuity loss and atrophic RPE lesions, in which small changes are measurable,

progress over time. Although this relationship may justify using RPE atrophy as a surrogate, there is a profound disconnect, particularly in late-onset Stargardt, between the area of RPE atrophy and vision. This discordance can be explained by clinically distinct progression subtypes: progression to either a foveal sparing phenotype in which RPE atrophy encircles the fovea in a horseshoe- or donut-like fashion (cohort III),^{7,8,10,22} or a subtype in which no such foveal sparing occurs (cohort IV). Foveal involvement can determine the eventual vision loss, either early when the eye has an initially involved fovea, or late when it exhibits a foveal sparing phenotype.

As discussed above, visual acuity can vary widely, and for now, unpredictably, depending on the eventual foveal involvement. As the present data show, a large group of 37% with foveal involvement will do poorly, the rest relatively well. To determine those patients that would benefit most from therapy in terms of future clinical trials, analysis of additional imaging modalities could be helpful. While mottled decreased areas are difficult to quantify,²¹ other imaging biomarkers, in particular, spectral-domain optical coherence tomography, could indicate what drives the disease process toward foveal involvement. It has been demonstrated that outer retinal involvement precedes RPE loss. Specifically, outer nuclear layer and ellipsoid zone thinning can occur in regions of normal RPE thickness, suggesting that photoreceptor thinning may precede RPE degeneration.²⁶ Hence, outer retinal damage on spectral-domain optical coherence tomography would precede recognition on FAF. In addition, environmental and genetic factors could significantly influence the development of RPE atrophy as identified in atrophic AMD.^{27,28} Such data were not included in this study and need to be addressed in future work.

Further limitations include the retrospective nature of the study and the resulting heterogeneity of the patients' data, which may have been the reason for failing to show significance between different subtypes of late-onset Stargardt. For instance, some patients did not report any symptoms, and were more likely to have no RPE atrophy or only extrafoveal RPE atrophy not encircling the fovea. These patients would need a longer follow-up to identify in which direction the disease will develop. Analogously, heterogeneity within the imaging data, for example, the fields of view in NIR and FAF imaging, might have led to the nondetection of more peripheral atrophic lesions in patients with a 30° field of view, while such lesions would have been detected in eyes imaged with a 55° objective.

In recent years, identifying biomarkers in retinal disease has become a central issue for therapeutic trials that aim to test the efficacy of a drug. A surrogate outcome measure accepted by the U.S. Food and Drug Administration is geographic atrophy in AMD,¹⁷ to which areas of RPE atrophy show close similarities. As this study now has shown that RPE atrophy can also be used as an outcome measure in late-onset Stargardt, it may even be valuable in other retinal diseases affecting the RPE. Of special interest is the precise characterization of late-onset Stargardt patients; their adult age makes them ethically more appropriate candidates to participate in clinical trials than patients who are of minor age. This study provides important knowledge on the natural history of late-onset Stargardt, quantitatively describing the course of visual loss and atrophy progression. In addition, it provides fundamental information necessary to conduct clinical trials in patients with Stargardt disease.

Acknowledgments

The authors thank Stéphanie S. Cornelis and Frans P.M. Cremers from the Department of Human Genetics, Donders Institute for Brain, Cognition and Behaviour, Radboud University Medical

Center, Nijmegen, The Netherlands, for their analysis of *ABCA4* mutations; and Joannes M. M. Groenewoud from the Department for Health Evidence, Donders Institute for Brain, Cognition and Behaviour, Radboud University Medical Center, Nijmegen, The Netherlands, for his statistical help and advice.

Supported by the Stichting A.F. Deutman Researchfonds Oogheelkunde, Nijmegen, The Netherlands; Nederlandse Oogonderzoek Stichting, Nijmegen, The Netherlands; Deutsche Forschungsgemeinschaft, Bonn, Germany, Grant No. FL 658/4-1 and Ho1926/3-1; BONFOR GEROK Program, Faculty of Medicine, University of Bonn, Grant No. O-137.0020; and the following foundations that contributed through UitZicht: Stichting MD fonds, Landelijke Stichting voor Blinden en Slechtzienden, and Oogfonds. The funding organizations had no role in the design or conduct of this research. They provided unrestricted grants.

Disclosure: **S. Lambertus**, None; **M. Lindner**, None; **N.M. Bax**, None; **M.M. Mauschitz**, None; **J. Nadal**, None; **M. Schmid**, None; **S. Schmitz-Valckenberg**, None; **A.I. den Hollander**, None; **B.H.F. Weber**, None; **F.G. Holz**, None; **G.J. van der Wilt**, None; **M. Fleckenstein**, None; **C.B. Hoyng**, None

References

- Blacharski PA. Fundus flavimaculatus. In: Newsome DA, ed. *Retinal Dystrophies and Degenerations*. New York, NY: Raven Press; 1988:135-159.
- Rotenstreich Y, Fishman GA, Anderson RJ. Visual acuity loss and clinical observations in a large series of patients with Stargardt disease. *Ophthalmology*. 2003;110:1151-1158.
- Fujinami K, Zernant J, Chana RK, et al. Clinical and molecular characteristics of childhood-onset Stargardt disease. *Ophthalmology*. 2015;122:326-334.
- Lambertus S, van Huet RA, Bax NM, et al. Early-onset Stargardt disease: phenotypic and genotypic characteristics. *Ophthalmology*. 2015;122:335-344.
- Westeneng-van Haaften SC, Boon CJ, Cremers FP, Hoefsloot LH, den Hollander AI, Hoyng CB. Clinical and genetic characteristics of late-onset Stargardt's disease. *Ophthalmology*. 2012;119:1199-1210.
- Fritsche LG, Fleckenstein M, Fiebig BS, et al. A subgroup of age-related macular degeneration is associated with monoallelic sequence variants in the *ABCA4* gene. *Invest Ophthalmol Vis Sci*. 2012;53:2112-2118.
- Sunness JS. The natural history of geographic atrophy, the advanced atrophic form of age-related macular degeneration. *Mol Vis*. 1999;5:25.
- Sunness JS, Gonzalez-Baron J, Applegate CA, et al. Enlargement of atrophy and visual acuity loss in the geographic atrophy form of age-related macular degeneration. *Ophthalmology*. 1999;106:1768-1779.
- Sarks JP, Sarks SH, Killingsworth MC. Evolution of geographic atrophy of the retinal pigment epithelium. *Eye (Lond)*. 1988;2(pt 5):552-577.
- van Huet RA, Bax NM, Westeneng-van Haaften SC, et al. Foveal sparing in Stargardt disease. *Invest Ophthalmol Vis Sci*. 2014;55:7467-7478.
- McBain VA, Townend J, Lois N. Progression of retinal pigment epithelial atrophy in Stargardt disease. *Am J Ophthalmol*. 2012;154:146-154.
- Han Z, Conley SM, Naash MI. Gene therapy for Stargardt disease associated with *ABCA4* gene. *Adv Exp Med Biol*. 2014;801:719-724.
- Schwartz SD, Hubschman JP, Heilwell G, et al. Embryonic stem cell trials for macular degeneration: a preliminary report. *Lancet*. 2012;379:713-720.
- Charbel Issa P, Barnard AR, Herrmann P, Washington I, MacLaren RE. Rescue of the Stargardt phenotype in *Abca4* knockout mice through inhibition of vitamin A dimerization. *Proc Natl Acad Sci U S A*. 2015;112:8415-8420.
- Cukras CA, Wong WT, Caruso R, Cunningham D, Zein W, Sieving P. Centrifugal expansion of fundus autofluorescence patterns in Stargardt disease over time. *Arch Ophthalmol*. 2012;130:171-179.
- Lois N, Halfyard AS, Bird AC, Holder GE, Fitzke FW. Fundus autofluorescence in Stargardt macular dystrophy-fundus flavimaculatus. *Am J Ophthalmol*. 2004;138:55-63.
- Csaky KG, Richman EA, Ferris FL III. Report from the NEI/FDA Ophthalmic Clinical Trial Design and Endpoints Symposium. *Invest Ophthalmol Vis Sci*. 2008;49:479-489.
- Schmitz-Valckenberg S, Brinkmann CK, Alten F, et al. Semi-automated image processing method for identification and quantification of geographic atrophy in age-related macular degeneration. *Invest Ophthalmol Vis Sci*. 2011;52:7640-7646.
- Boon CJ, van Schooneveld MJ, den Hollander AI, et al. Mutations in the peripherin/RDS gene are an important cause of multifocal pattern dystrophy simulating STGD1/fundus flavimaculatus. *Br J Ophthalmol*. 2007;91:1504-1511.
- Boon CJ, Klevering BJ, Cremers FP, et al. Central areolar choroidal dystrophy. *Ophthalmology*. 2009;116:771-782.
- Kuehlewein L, Hariri AH, Ho A, et al. Comparison of manual and semiautomated fundus autofluorescence analysis of macular atrophy in Stargardt disease phenotype. *Retina*. 2016;36:1216-1221.
- Lindner M, Boker A, Mauschitz MM, et al. Directional kinetics of geographic atrophy progression in age-related macular degeneration with foveal sparing. *Ophthalmology*. 2015;122:1356-1365.
- R Development Core Team. R: A Language and Environment for Statistical Computing. Vienna, Austria: R Foundation for Statistical Computing. 2012. Available at <http://www.R-project.org/>. Accessed June, 18, 2015.
- Turnbull BW. The empirical distribution function with arbitrary grouped, censored and truncated data. *J R Stat Soc Series B Stat Methodol*. 1976;38:290-295.
- Dreyhaupt J, Mansmann U, Pritsch M, Dolar-Szczasny J, Bindewald A, Holz FG. Modelling the natural history of geographic atrophy in patients with age-related macular degeneration. *Ophthalmic Epidemiol*. 2005;12:353-362.
- Burke TR, Rhee DW, Smith RT, et al. Quantification of peripapillary sparing and macular involvement in Stargardt disease (STGD1). *Invest Ophthalmol Vis Sci*. 2011;52:8006-8015.
- Finger RP, Chong E, McGuinness MB, et al. Reticular pseudodrusen and their association with age-related macular degeneration: the Melbourne Collaborative Cohort Study. *Ophthalmology*. 2016;123:599-608.
- Reynolds R, Rosner B, Seddon JM. Dietary omega-3 fatty acids, other fat intake, genetic susceptibility, and progression to incident geographic atrophy. *Ophthalmology*. 2013;120:1020-1028.